Journal of Materials and Environmental Science
ISSN : 2028-2508
e-ISSN : 2737-890X
CODEN : JMESCN

J. Mater. Environ. Sci., 2024, Volume 15, Issue 1, Page 136-150

http://www.jmaterenvironsci.com

Experimental, Quantum chemical and IR spectroscopy studies on the corrosion inhibition of mild steel by 3,5-dimethyl-4-nitroisoxazole in HCl solutions

Essien, K. E.[1*], Okon, E. J.[2], Archibong, I. N.[3], Okon, O. E.[2], George, I. E.[2]

[1]*Department of Chemistry, Faculty of Physical Sciences, Akwa Ibom State University, Mkpat Enin, P.M.B. 1167, Nigeria*
[2]*Department of Chemical Sciences, Akwa Ibom State Polytechnic, Ikot Osurua, P.M.B. 1200, Nigeria*
[3]*Department of Chemistry, Faculty of Sciences, College of Education, Afaha Nsit, P.M.B., Nigeria*
** Corresponding author, Email address: kufreessien@aksu.edu.ng*

Received *18 Dec 2023,*
Revised *13 Jan 2024,*
Accepted *18 Jan 2024*

Keywords:
- ✓ *3,5-dimethyl-4-nitroisoxazole;*
- ✓ *Quantum;*
- ✓ *Mild steel;*
- ✓ *Enthalpy;*
- ✓ *Adsorption*

Citation*: Essien K.E., Okon E. J., Archibong I.N., Okon O.E., George I.E. (2024). Experimental, Quantum chemical and IR spectroscopy studies on the corrosion inhibition of mild steel by 3,5-dimethyl-4-nitroisoxazole in HCl solutions, J. Mater. Environ. Sci., 15(1), 136-150*

Abstract: The gravimetric, quantum and surface characterization methods were used to examine anticorrosion potential of the 3, 5-dimethyl-4-nitroisoxazole (DNI) for mild steel in a 2M HCl solution at the temperature range of 30°C – 60°C. The results obtained revealed that inhibition efficiency increased with an increase in inhibitor concentrations ranging from $2x10^{-4}$ M to $10x10^{-4}$ M. The maximum inhibition at the optimum concentrations of DNI in HCl solution at 30°C was 71 %. The negative values of Gibb's free energy (ΔG^{o}_{ads}) ranged from -14.52 kJ/mol to -22.57 kJ/mol indicating spontaneous adsorption of the inhibitors on a mild steel surface, and the adsorption mechanism is physisorption. The positive values of ΔH° reflect the endothermic behavior of the adsorption of the studied inhibitor on the mild steel surface. The negative values for entropy imply that the adsorption process is accompanied by a decrease in entropy. Fukui index was proposed to foresee electrophilic and nucleophilic sites of the inhibitor molecule. The Fourier transformed infra-red spectrophotometer was used to identified the functional groups participating in the inhibition process. Some functional groups of the inhibitor disappeared while some were re-characterized by shifts in frequency of absorption. FTIR results confirm the adsorption of DNI molecule on the mild steel surface.

1. Introduction

The corrosion process is a phenomenon that revolves around the utilized acid (HCl, H_2SO_4 or H_3PO_4), the concentration of the acid, the flow velocity, the absolute temperature, and the existence of dissolved inorganic or organic elements which constitute a complication for its distended applicability (Sastri, 2012; Zarrok *et al.*, 2012). For instance, acids as media are employed in methods such as decalcification, acidification, and pickling of oil, in the detriment of inorganic-metal components corrosion (El-Etre, 2008). From the perspectives of tragic accidents together with loss of life, corrosion is very critical. Corrosion phenomenon is considered in a very critical way from the viewpoint of safety, environmental impact and economics. The economic sides of corrosion are extremely beyond what most people realize. The survey carried out by the NACE-NBS (National Association of Corrosion EngineersNational Bureau of Standards), the overall cost of corrosion in Canada is valued at approximately 2.5% of their total GDP, emphasizing the costs of handling

corrosion effects, not merely the safety and environmental mischief of corrosion, in a global society. According to a 2001 report, the expenditure on corrosion in the U.S. alone was $276 billion per year. Of this, about $121 billion was spent to control corrosion, leaving the difference of $155 billion as the net loss to the economy.

On the other hand, the protection of the transition metal-surface against dissolution with the organic compounds remained the upmost efficacious and economical method. The inhibition of corrosion in several acidic media may be ensured by adding a variety of organic inhibitory compounds containing electronegative functional groups (i.e., C=O, =N-N=, =N-C…etc.) and π-π systems in conjugated double or triple links, which indeed exhibit satisfactory inhibiting properties by supplying electrons through π-π orbitals (Le Goff and Ouazzani, 2014; Hosseini, 2007; Thoume *et al.*, 2020). However, the employment of organic inhibitors in aggressive environments can, in some cases, induce the exaltation of the inorganic-metal corrosion (Solomon et al., 2020). Many azole derivatives such as oxazole (Solomon et al., 2020), pyrazole (Glaser *et al.*, 2000; El Ouafi *et al.*, 2002; Tebbji *et al.*, 2007; Yadav *et al.*, 2016) and Benzimidazole (El Arrouji *et al.*, 2016; El Arrouji *et al.*, 2020) compounds have been recently studied as corrosion inhibitors for mild steel in hydrochloric acid, and have been shown exhibited good inhibition properties.

In the current paper, we are to investigate the corrosion inhibition properties of 3, 5-dimethyl-4-nitroisoxazole in 2 M HCl by using gravimetric, computational and IR method of analyses. The study of 3, 5-dimethyl-4-nitroisoxazole was due to its accomplishment of the crucial requirements of corrosion inhibitors as reported by Umoren (2008). Moreover, it has not been used as mild steel corrosion inhibitor in Hydrochloric acid to the best of our knowledge. The study shall involve investigating anti-corrosion potential of the 3, 5-dimethyl-4-nitroisoxazole for mild steel in an acidic medium. It is also likely that with the various adsorption sites, complexes will be formed with the metal ions and on the metal surface (Umoren, 2011). A thin protective layer built up by the organic compound on the metal surface protects the metal from the corrosive attack of the surroundings by bringing down the corrosion rate (Chauhan *et al.*, 2021; Azzaoui *et al.* 2017; Abboud *et al.* 2009). A comparative work was performed to inspect the inhibition activity of this derivative in connection with their molecular geometries (extent of planarity), global and local electronic properties in a destructive acid aqueous medium. Furthermore, their deformation capacity to adhere to the mild steel surface was investigated through the calculations supported by the DFT method of the 3, 5-dimethyl-4-nitroisoxazole (DNI) (Figure 1).

This work shall aid in the assimilation of corrosion mechanisms and minimize corrosion setback. The 3, 5-dimethyl-4-nitroisoxazole is a product of Sigma Aldrich, and the structure is shown in Figure 1.

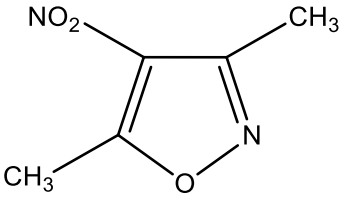

Figure 1: Chemical Structure of 3, 5-dimethyl-4-nitroisoxazole

2. Methodology

2.1 Gravimetric experiments

The various concentrations of 3, 5-dimethyl-4-nitroisoxazole were prepared using 2 M HCl solution. The coupons with dimension of 5 x 4 cm were immersed in 100 ml test solutions

maintained at 303 – 333 K. The experiment was performed on mild steel coupons after being polished with SiC abrasive papers and degreased in absolute ethanol, dried in acetone and store up in moisture-free desiccators before use (Oguzie *et al.*, 2012). The examination of weight loss measurement was considered by retrieving the coupons from test solutions at 2 h intervals progressively for 10 h, washing in zinc dust solution with a bristle brush, rinsing in distilled water, drying in acetone, and re-weighed (Oguzie *et al.*, 2012). The difference between the initial weight and the weight of the coupons at a given time interval was considered as the weight loss.

2.2 Molecular modeling

The PM7 Hamiltonian in the MOPAC 2014 software was used in computing semi-empirical parameters for the molecule (Ebenso *et al.*, 2010). TheFull optimization was done using molecular mechanics, *Ab initio*, and DFT level (Eddy *et al.*, 2015). Single point DFT calculations were also carried out using Hyperchem release 8.2 packages. DFT setting (MP2 inclusive) in the package were, Basic set: 321-G, iteration = 50, spin pairing = unrestricted Hartree Fock, convergence limit = 1E-0.05 and Spin multiplicity = 1 (for zero charge and 2 for +1 and -1 charges). The relation between the inhibition efficiency of this inhibitor and the quantum chemical parameters was considered (Eddy *et al.*, 2010). The corrosion inhibition mechanisms were studied using quantum chemical calculations, and the probable physical properties were determined to know which could make the inhibition possible.

2.3 Surface Characterization

The microstuctural features were identified by using Fourier Transform Infra Ray (FT-IR), and the coatings were studied to interpret the results of corrosion tests. The surfaces of the corroded samples were observed after 24 h of immersion in the respective corrosive medium. The IR spectra were recorded for the DNI solution and 2.0 M HCl solution after 24 h of mild steel sample immersion at 303 K. The mild steel was retrieved and scraped out the corrosion products from the surface for the test.

3. Results and Discussion

3.1 Weight loss studies

To minimize the corrosion of mild steel in the acidic medium, the gravimetric experiment was carried out by using the 3, 5-dimethyl-4-nitroisoxazole (DNI) as the inhibitor (Ebenso *et al.*, 2010), pyrazole (Eddy *et al.*, 2015; Eddy *et al.*, 2010). The weight loss measurement was observed to increase with an increase in time but decrease with an increase in concentrations of the 3, 5-dimethyl-4-nitroisoxazole (Table 1). A similar trend was observed by many researchers (Umoren, 2008), pyrazole (Kousar *et al*., 2021; Khaled *et al*., 2012; Obi-Egbedi *et al*., 2011; Obot *et al*., 2010; Tang *et al*., 2006; Obot *et al*., 2008). Figure 2 showed the weight loss measurements with time at 30^{o} C and related trends were observed at 40, 50, and 60^{o} C. An increase in corrosion rates with contact time for all systems and a decrease in corrosion rates due to the addition of the studied inhibitor is shown in figure 2. This indicates the retardation of the mild steel corrosion in the corrosive environment (Njoku *et al.*, 2019; Jackson and Essien, 2019; Ghazoui *et al.*, 2013). A similar result was reported by Paul *et al.* (2019).

The studied compound exhibits corrosion-inhibiting effects at all concentrations reaching a maximum inhibition efficiency of 71 % at the optimum concentration of 10 x 10^{-4} M (Table 1). The studied inhibitor was found to be more efficient at 303 K (Table 1) (Hosseini *et al.*, 2010). This result

corresponds to that of Paul *et al.* (2019), Essien *et al.* (2022) and Dohare *et al.* (2019) which is attributed to partial desorption of the molecules from the Mild Steel surface.

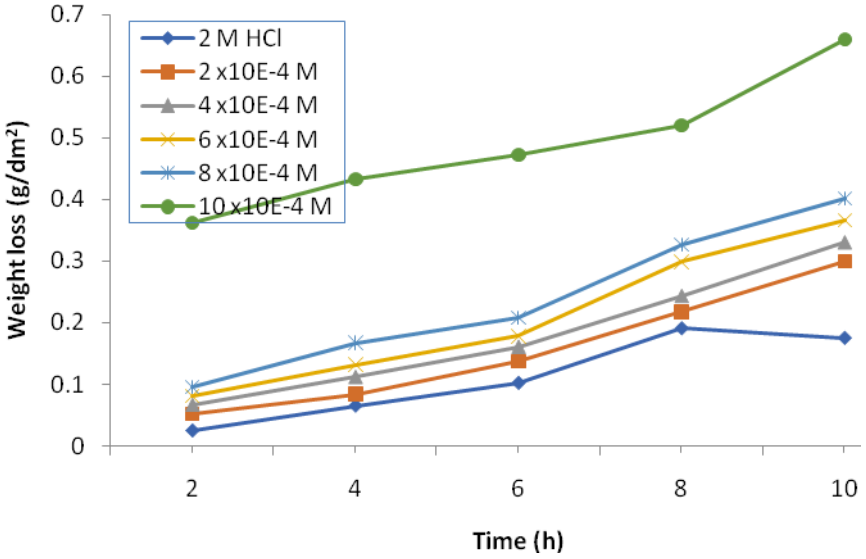

Figure 2: Plot of weight loss versus time (h) in the absence and presence of different concentrations of DNI at 30^0C.

Table 1: Calculated values of corrosion rate (CR), surface coverage (θ) and inhibition efficiency (%I) of mild steel corrosion in different concentration of DNI

	303 K			**313 K**			**323 K**			**333 K**		
Conc. of [DNI] (M) x 10^{-4}	CR (mm/yr) x 10^3	θ	I (%)	CR (mm/yr) x 10^3	θ	I (%)	CR (mm/yr) x 10^3	θ	I (%)	CR (mm/yr) x 10^3	θ	I (%)
Blank	3.00	-	-	4.96	-	-	6.34	-	-	8.41	-	-
2	2.01	0.33	33	3.82	0.23	23	5.01	0.21	21	7.57	0.10	10
4	1.83	0.39	39	3.57	0.28	28	4.69	0.26	26	7.23	0.14	14
6	1.65	0.45	45	3.17	0.36	36	4.57	0.28	28	6.81	0.19	19
8	1.50	0.50	50	2.93	0.41	41	4.38	0.31	31	6.56	0.22	22
10	0.88	0.71	71	2.53	0.49	49	3.93	0.38	38	6.06	0.28	28

3.2 Effect of temperature

To understudy the temperature dependence of corrosion rates in uninhibited and inhibited solutions, the gravimetric measurements were carried out in the temperature range 303 K – 333 K in the presence of different concentrations of DNI in 2 M HCl solutions (Dohare *et al.*, 2019; Ozoemena *et al.*, 2023). The inhibition efficiencies as a function of concentrations are presented in table 1. The results show that inhibition efficiency increased with the concentration of inhibitor (Fouda *et al.*, 2006; salim *et al.*,2016). Similar behavior was reported by many researchers (Eddy *et al.*, 2015; Dohare *et al.*, 2019; Jackson *et al.*, 2016; Verma *et al.*, 2020; Ouchrif *et al.*, 2005; El Ouadi *et al.*, 2021). High efficiency of 71 % was noticed after 10 h, which points out, that the surface coverage of the substrate by these inhibitors attended an optimum level within 10 h. From the results, the highest concentration of this inhibitor at 303 K gives maximum inhibition efficiency. The results show that inhibition efficiency decreases as the temperature increases indicating the physisorption process as reported by Khaled *et al.* (2012). From the results, it could be observed that inhibitor concentration increases as the corrosion rate decreases, thus leading to an increase in the inhibition efficiency.

Careful investigation performed for Temkin, Langmuir, Frumkin and Freundlich isotherms (equations 1-4) would show the most fitting isotherm with maximum regression coefficients, R2, using the following relationships:

Temkin isotherm $\exp(f.\theta) = K_{ads} C$ (1)

Langmuir isotherm $\theta / (1- \theta) = K_{ads} C$ (2)

Frumkin isotherm $\theta / (1- \theta) . \exp(-2f.\theta) = K_{ads} C$ (3)

Freundlich isotherm $\theta = K_{ads} C$ (4)

where K_{ads} is the equilibrium constant of the adsorption process, C is the inhibitor concentration and f the heterogeneous factor of metal surface.

The adsorptions of this inhibitor on mild steel surfaces were studied using adsorption isotherms (figures 3a and 3b) (Obot *et al*., 2010; Obi-Egbedi *et al*., 2011; Essien *et al*., 2022). Adsorption isotherms gave vital information on the interaction of inhibitor and metal surfaces as observed by Umoren (2008). The degree of surface coverage values (θ) at different inhibitor concentrations in 2 M HCl solutions were assessed from weight loss measurements at 303 K – 333 K and tested graphically for fitting to a suitable adsorption isotherm (Tang *et al*., 2006; Jackson and Essien, 2019; Jackson *et al*., 2016). The adsorption isotherm model considered was Temkin isotherm (Figure 3a) as reported by Obot and Obi-Egbedi (2011 & 2008). The best-fitted straight line in all the adsorption isotherm models considered was in the Temkin isotherm (figure 3a) with correlation coefficients (R2) ranging from $0.9977 \geq R2 \geq 0.9304$. The values of molecular interaction parameter 'a' shown in table 2 are negative in all cases which implies attraction in the adsorption layer. A similar result was observed by Obot and Obi-Egbedi (2008). It is obvious from table 2 that, the values of K_{ads} are very low indicating weak interaction between the inhibitor and the mild steel surface which implies the electrostatic interaction (Physisorption) between the inhibitor molecules and the metal surface (Abd El Rehim *et al*., 2001). The negative values of $\Delta G°_{ads}$ indicates spontaneous process (Jackson and Essien, 2019; Fouda *et al*., 2006; Jackson *et al*., 2016).

Table 2: Adsorption parameters from Temkin isotherm for Mild steel coupons in 2M HCl containing different concentration of DNI at 30-60°C.

Temp. (°C)	**Adsorption parameters**						
	Intercept	Slope	K_{ads} (mol/l)	f	a	$-\Delta G°_{ads}$ (kJ/mol)	R^2
30	0.223	0.069	25.28	14.49	-7.25	18.25	0.9977
40	0.159	0.065	11.59	15.39	-7.70	16.83	0.9937
50	0.171	0.039	80.64	25.64	-12.82	22.57	0.9578
60	0.054	0.044	3.42	22.73	-11.37	14.52	0.9918

The activation energy values in Table 3 indicate that the presence of DNI increases the activation energy of the metal dissolution reaction. The adsorption of the studied inhibitors is believed to take place on the higher energy sites and the presence of the inhibitor, which results in the blocking of the active sites, must be related to an increase in the activation energy of mild steel corrosion in the inhibited state (Soltani *et al*., 2014). The higher value of E_a in the presence of inhibitors compared to that in its absence and the decrease in the inhibition efficiency (%) with rising in temperature is deduced as an indication of physisorption.

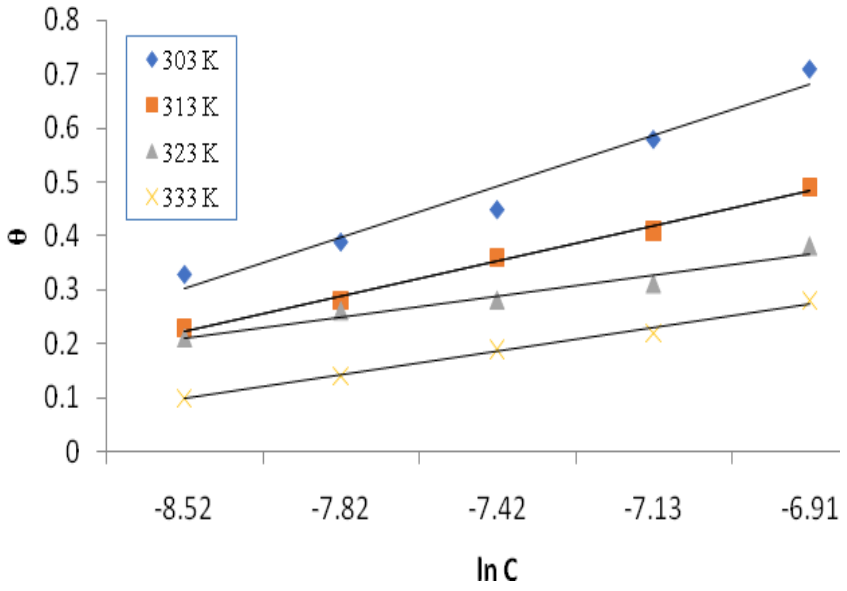

Figure 3a: Temkin adsorption isotherm plot as θ versus ln C for Mild steel coupons in 2M HCl solution containing different concentrations of DNI.

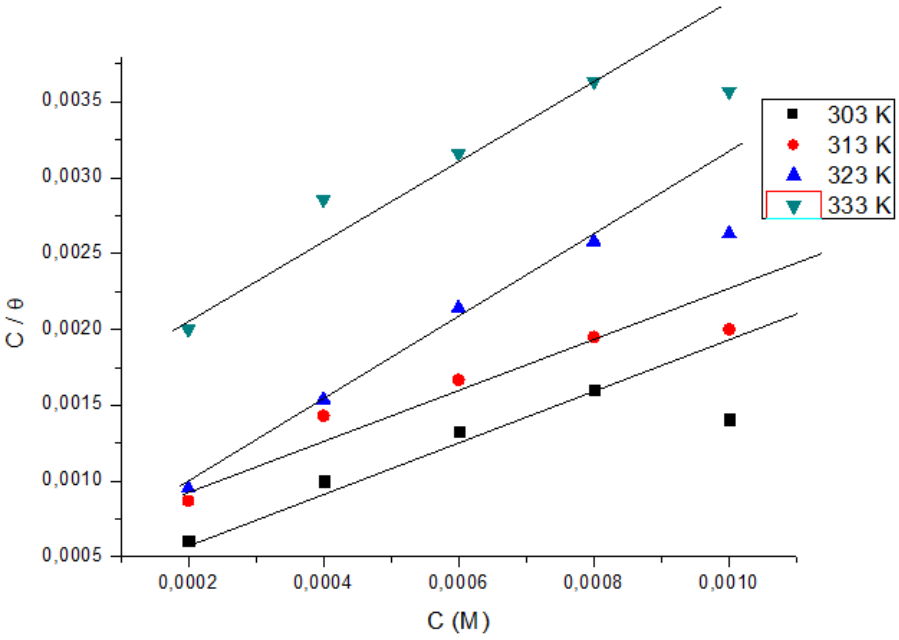

Figure 3b: Langmuir adsorption isotherm plot as C/θ versus C for Mild steel coupons in 2M HCl solution containing different concentrations of DNI.

The transition state plot is presented in figure 5 (Solomon *et al.*, 2022; Jackson *et al.*, 2016). The computed values of the activation parameters for the dissolution of mild steel at different temperatures are presented in table 3. Examination of these data in table 3 revealed that the positive values of ΔH^o reflect the endothermic behavior of the adsorption of the studied inhibitor on the mild steel surface (Tang *et al.*, 2006; Essien and Abai, 2022). The ΔS^o values are negative indicating that the adsorption is an endothermic process (Tang *et al.*, 2006; Jackson and Essien, 2019; Essien and Abai, 2022). The adsorption between the organic compound in the aqueous phase [org (sol)] and water molecules at the electrode surface [$H_2O_{(ads)}$] is regarded as a quasi-substitution process (Fouda

et al., 2006; Essien *et al.*, 2023). Thus, the adsorption of DNI is accompanied by desorption of water molecules from the electrode surface.

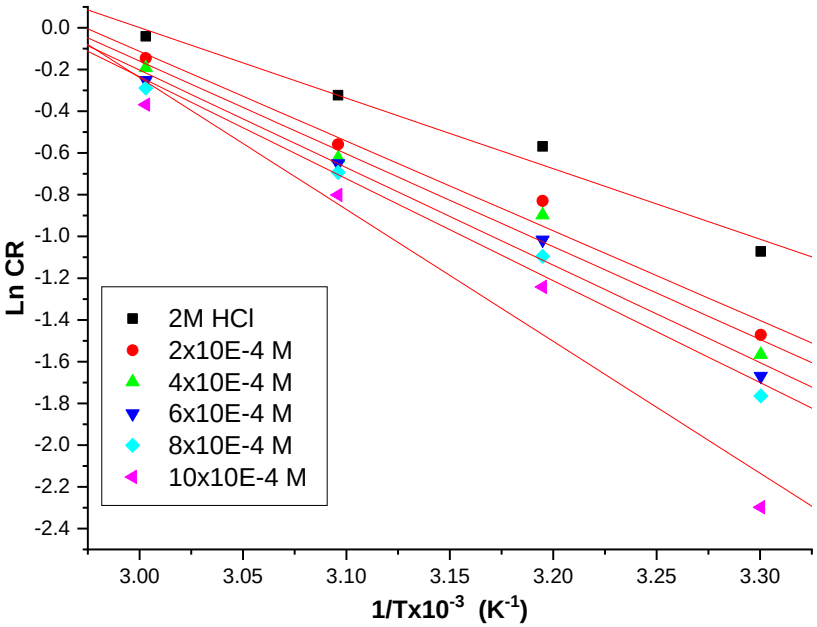

Figure 4: Arrhenius plot as log CR versus 1/T for mild steel coupons in 2 M HCl containing different concentrations of DNI.

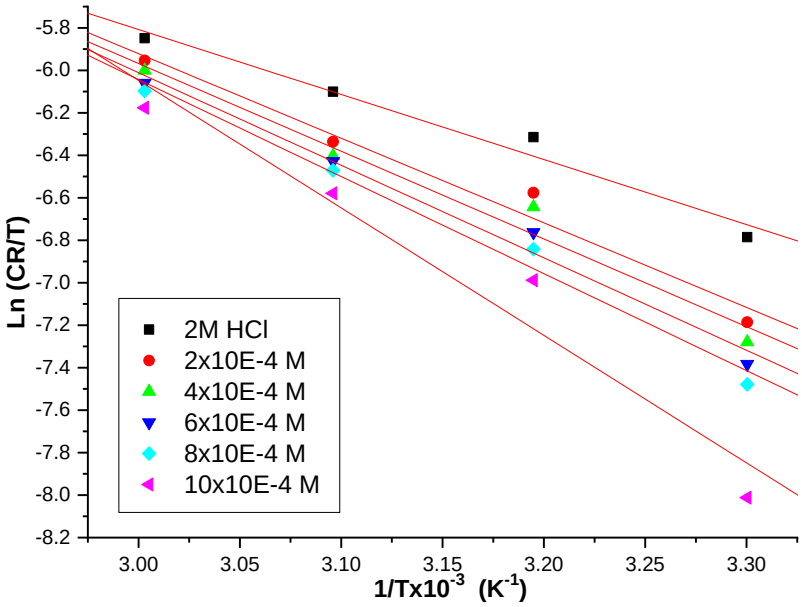

Figure 5: Transition State plot as log (CR/T) versus 1/T for mild steel coupons in 2 M HCl containing different concentrations of DNI.

The difference (E_a - ΔH) agrees the known thermodynamic equation :

$E_a - \Delta H = RT$

The obtained values quite equal 2.64 kJ/mol to RT = 8.314*318 where 318 K is the mean temperature studied. This equation reveals that reduction of hydrogen ion passes first to unimolecular atom H_{ads} to be combined after to H_{ads} to H_2 (Zarrouk *et al.*, 2011; Hammouti *et al.*, 2011).

Table 3: Activation parameters for Mild steel in 2 M HCl containing different concentrations of DNI at 30-60^{o}C.

DNI Conc. (M) x 10^{-4}		**Activation parameters**			
	Ea (kJ/mol)	ΔH (kJ/mol)	ΔS (J/mol K^{-1})	A (mm/yr) x 10^{3}	Ea - ΔH (kJ/mol)
Blank	28.12	25.48	-169.55	2.54E+04	2.64
2	35.77	33.13	-147.54	3.57E+05	2.64
4	36.99	34.36	-144.26	5.30E+05	2.63
6	38.88	36.24	-138.95	1.00E+06	2.64
8	40.65	38.01	-133.92	1.84E+06	2.64
10	52.59	49.95	-98.13	1.36E+08	2.64

Consequently, the adsorption process is endothermic and associated with a decrease in entropy of the solute; the same is factual for the solvent. The thermodynamic parameters obtained are the algebraic sum of the adsorption of these organic molecules and desorption of water molecules (Soltani *et al.*, 2014). Thus, the increase in entropy is due to the increase in solvent entropy (Emranuzzaman *et al.*, 2004). The negative values for entropy imply that the adsorption process is attended by a decrease in entropy, which is the driving force for the adsorption of DNI on the mild steel surface (Li *et al.*, 2014).

3.3 Global molecular reactivity

The MOPAC 2014 software was used to compute the quantum chemical parameters (Table 4). Similar software has been used by Eddy *et al.* (2011) and Essien & Abai (2022). The HOMO and LUMO molecular orbitals of the 3,5-dimethyl-4-nitroisoxazolemolecule are shown in figures 6 and 7 respectively. The blue and maroon orbital represent positive and negative sites of adsorption respectively. The reactivity of a chemical species can be defined as the difference in energy of the highest occupied molecular orbital (E_{HOMO}) and that of the lowest unoccupied molecular orbital (E_{LUMO}).

The smaller the energy gap, the higher reactivity of the chemical species (Jackson and Essien, 2019; Eddy, 2011; Hmamou *et al.*, 2013; Hayaoui, *et al.*, 2017). From Table 4, it is obvious that the energy gap, ΔE of the studied inhibitor is 9.78 eV. As a result, the inhibition efficiency of the inhibitor molecule is 71 %. Figures 6 and 7 showed the distribution of HOMO and LUMO of 3, 5-dimethyl-4-nitroisoxazole molecule, and it could be seen that the distribution of HOMO and LUMO is mainly located at the oxazole ring, nitrogen, and oxygen atoms in substituent groups. This kind of distribution favors the parallel adsorption of oxazole derivative inhibitor onto the metal surface (Solomon *et al.*, 2022; Yadav *et al.*, 2014). This implies that the inhibitor molecules donate electrons to the unoccupied d orbital of the Fe atom forming a coordinate bond and the inhibitor molecules accept electrons from the Fe atom to form a back-donating bond (Deng *et al.*, 2014).

The ionization energy was estimated through the value of E_{HOMO} with Semi-empirical calculations. In this case, two systems, Fe (in mild steel) and inhibitor are brought together, hence, electrons will flow from the lower system with lower electronegativity (inhibitor) to the system with higher electronegativity until the chemical potential becomes equal (Ebenso *et al.*, 2010; Eddy, 2011). The trend for the variation of inhibition potentials of the studied oxazole derivative agrees with experimental findings. The hydrophobicity of the actual molecule is accounting for by the substituent

Log P. The hydrophobicity of organic molecule increases with decreasing water solubility. In corrosion studies, hydrophobicity is related to the mechanism of formation of the oxide/hydroxide layer on the metal surface (which reduces the corrosion process drastically) (Eddy, 2011; Obot *et al.*, 2021).

Table 4: PM7 semi empirical parameters for the studied 3, 5-dimethyl-4-nitroisoxazole molecule

Semiempirical Parameters (eV)	DNI
H_f (kCal/mol)	-2.01
TE (eV)	-1949.18
EE (eV)	-8790.44
CCR (eV)	6841.26
Dipole (eV)	2.47
IE (eV)	10.95
E_{HOMO} (eV)	-10.95
E_{LUMO} (eV)	-1.17
E_{L-H} (eV)	9.78
Cosmo area ($Å^2$)	159.24
Cosmo volume ($Å^3$)	154.48
Hydration energy (kCal/mol)	-8.77
LogP	-1.77
Refractivity ($Å^3$)	34.47
Polarizability ($Å^3$)	12.40

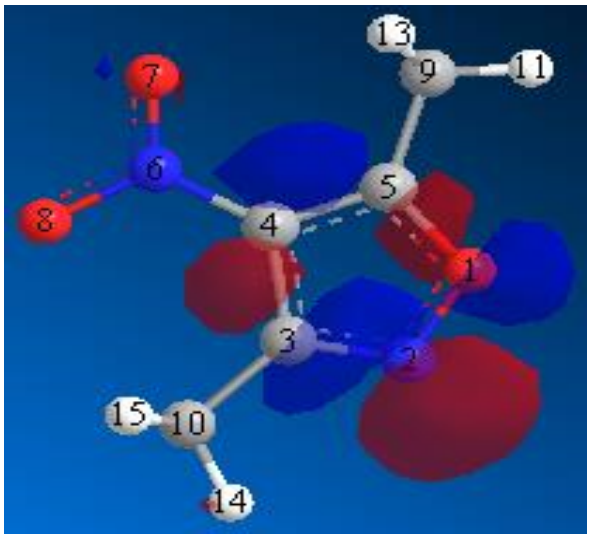

Figure 6: HOMO electronic density of DNI molecule

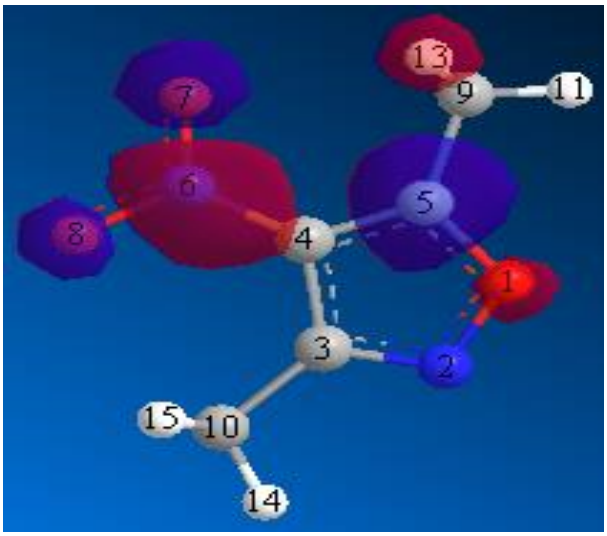

Figure 7: LUMO electronic density of DNI molecule

The dipole moment is the measured polarity of a polar covalent bond (Eddy, 2010). From table 4, the negative total energy indicates that the studied inhibitor is a very stable molecule and is less prone to be broken apart. The dipole moment of the studied inhibitor is 2.47 Debye which is higher than that of H_2O (1.87 Debye) (Eddy, 2010; Essien and Abai, 2022). The high values of dipole

moment probably increase the adsorption between the compound and metal surface (Ikot *et al.*, 2009). Moreover, effective adsorption of the studied molecules on the mild steel surface is enhanced by higher area and volume. Literature discloses that there are several abnormalities in the correlation involving dipole moment and inhibition efficiency, noting that core-core repulsion (C–C) energy is a quantum chemical parameter that has a tremendous correlation with inhibition efficiency (Eddy, 2010).

3.4 Local molecular selectivity

The condensed softness functions and condensed Fukui was used to determine the local molecular selectivity of the 3,5-dimethyl-4-nitroisoxazole molecule (Ebenso *et al*., 2010; Essien and Abai, 2022; Eddy, 2011). Table 5 showed the local reactivity parameters of the studied inhibitor. The fact that an electron is transferred to an N electron molecule gives rise to Fukui function. It tends to distribute to minimize the energy of the resulting N + d electron system (Essien and Abai, 2022; Eddy, 2011; Ikot *et al.*, 2009; Yadav *et al.*, 2014). The nucleophilic and electrophilic attack comes as a result of electron density change. The calculated values of f^+ and f^- for carbon, nitrogen, and oxygen atoms in DNI molecule are shown in Table 5. The nucleophilic and electrophilic attack sites is at the place where the values of f^+ and f^- are maximum. The metal surface would have strong contact with an atom with high f^+ and f^- by exchanging electrons (Eddy, 2011). From the f^+ and f^- presented in table 5, the active sites could be found. As for electrophilic attack index f^+, the active sites of inhibitor DNI are mainly located on N(2), O(8) and O(7). As for nucleophilic attack f^- of the studied inhibitor, the active sites are located mostly on the heteroatoms in the substituent groups (Dohare *et al.*, 2019; Eddy, 2011).

Table 5: Fukui functions for carbon and electronegative elements in 3,5-dimethyl-4-nitroisoxazole

Atom No.	q_{Huckel}	q_N	q_{N-1}	q_{N+1}	f_k^-	f_k^+	$f^{(2)}(r)$
O(1)	0.0626898	0.0323	0.0908	-0.0217	-0.0585	-0.0540	0.0045
N(2)	-0.221786	0.0465	0.1955	-0.0237	-0.1490	-0.0702	0.0788
C(3)	0.152824	-0.0414	0.0126	-0.0820	-0.0540	-0.0406	0.0134
C(4)	-0.0953987	0.0583	0.0734	0.0217	-0.0151	-0.0366	-0.0215
C(5)	0.296654	0.0386	0.0840	-0.0206	-0.0454	-0.0592	-0.0138
N(6)	1.24666	0.0724	0.1248	0.0596	-0.0524	-0.0128	0.0396
O(7)	-0.526779	-0.0437	0.0974	-0.1512	-0.1411	-0.1076	0.0335
O(8)	-0.938937	-0.0482	0.1012	-0.1713	-0.1494	-0.1231	0.0263
C(9)	-0.075342	-0.1038	-0.1241	-0.0979	0.0203	0.0059	-0.0144
C(10)	-0.0767933	-0.0886	-0.1165	-0.0852	0.0279	0.0035	-0.0244

The Fukui function is an effective parameter to describe the local reactivity (Deng *et al.*, 2014). From the results in Table 5, it could be seen that some atoms possessed both high f^+ and high f^-, and it meant that these atoms had strong capability to attract and donate electrons (Dohare *et al.*, 2019). A dual descriptor was used to estimate their contribution to exchanging electrons with the metal surface. The values of f^2 (r) for the studied molecule are presented in Table 5. This indicated that N(2), N(6) and O(7) are the electrophilic sites with f^2 (r) of 0.0788, 0.0396 and 0.0335 respectively. These three atoms accepted electrons from the metal surface, whereas C(4) and C(10) are the nucleophilic sites with f^2 (r) of -0.0215 and -0.0244 respectively.

3.5. Surface Characterization

It is established that IR spectroscopy can be utilized to understand the process of rusting of steels. FT-IR spectrum of surface film on mild steel immersed in the presence and absence of MPC is shown in Figure 8. The results revealed that the mild steel corrosion products in the presence of DNI are IR active.

It has been pointed out that the adsorption band at higher wavenumber region is due to OH stretching and at lower wave number region is because of Fe-O lattice vibration (Misawa *et al.*, 1974; Misawa *et al.*, 1971). Moreover, it is also showed that if this peak is sharp, it indicates the purity level and the prevalence of very small amount of defects (Ganesan *et al.*, 2020). From the results, it can be seen that the C-Cl band at 722.11 cm^{-1} in 2M HCl spectrum was shifted to 722.24 cm^{-1} in DNI. The C-H stretching band at 2922.75 cm^{-1} in 2M HCl was shifted to 2965.04cm^{-1} DNI spectra.
By comparing the spectra of adsorbed film with that of DNI inhibitor, we can conclude that some peaks have shifted to higher frequency region. The presence of these bands in the surface film indicates the existence of DNI molecule in the surface film. The shifts in the stretching frequencies of various functional groups present in the inhibitor molecules are resulted due to the involvement of the molecules in the complex formation. Similarly, the bands at 3419.5cm^{-1} in 2 M HCl and 3626.8 cm^{-1} in DNI IR spectra is contributed by the –OH group present in possibly traces of ferric hydroxide present in the inhibited film. Ishii and Nakahira (1972) also confirmed that the Fe-O stretching vibration in $Fe_{3-x}O_4$ corresponds to wave number, 400-600 cm^{-1}. Thus, the FT-IR spectrum of the surface film formed in presence of the inhibitor formulation infers the presence of [Fe(ll)-Inhibitor] complex and small amounts of oxides and hydroxides of Fe(lll). The disappearance and the shift of certain peaks to higher wave numbers clearly proved that some interactions have been taking place over the metal surface (Eddy *et al.*, 2010).

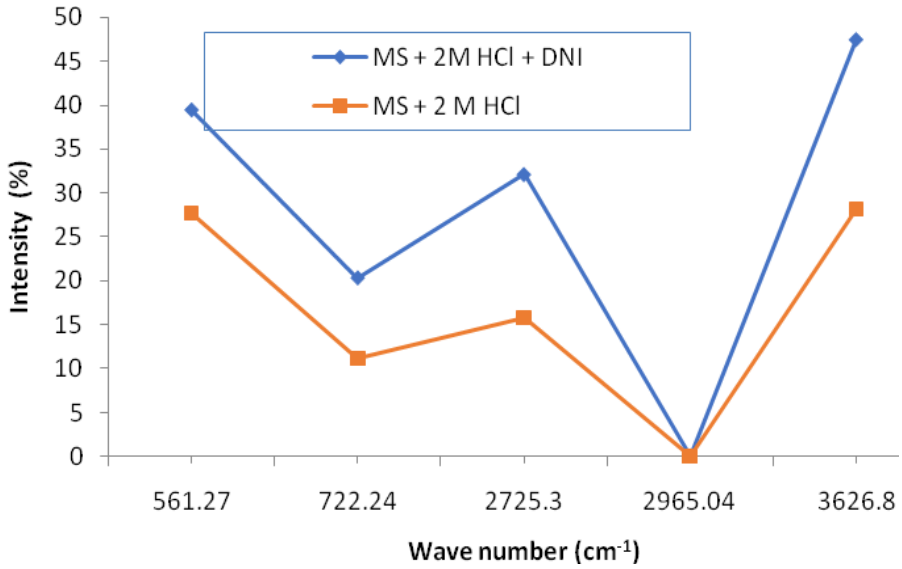

Figure 8: IR spectrum for mild steel (MS) after corrosion in 2 M HCl solution without and with 10 x 10^{-4} M DNI

Conclusion

The 3,5-dimethyl-4-nitroisoxazole molecule was more efficient in a 2 M HCl solution at 303 K. The thermodynamics parameters proposed physisorption process. The weight loss data fit most in Temkin adsorption isotherm. Quantum chemical calculations revealed that the studied compound adsorb both as cationic species and as molecular species using oxygen, nitrogen and carbon as its active centers.

The local molecular reactivity was used to evaluate the active sites of the inhibitor molecule. FT-IR spectroscopy was utilized to understand the process of rusting of mild steel. The FT-IR spectrum of the surface film formed in presence of the inhibitor formulation infers the presence of [Fe(ll)-Inhibitor] complex and small amounts of oxides and hydroxides of Fe(lll).

Compliance with ethical standards

Acknowledgments

The authors wish to express deep appreciation to the Akwa Ibom State University, Mkpat Enin, Nigeria for providing facilities for this study.

Disclosure of conflict of interest

The authors declare no conflicts of interest.

References

Abboud Y., Abourriche A., Tanane O., *et al.* (2009), Corrosion inhibition of carbon steel in acidic media by Bifurcaria bifurcata extract, *Chem. Eng. Comm.* 196 N°7, 788-800.

Abd El Rehim, S.S., Ibrahim, M.A. and Khalid, K.F. (2001). The inhibition of 4-(2′-amino-5′-methylphenylazo) antipyrine on corrosion of mild steel in HCl solution, *Mater. Chem. Phys*. 70, 268–273. https://doi.org/10.1016/S0254-0584(00)00462-4

Azzaoui, Mejdoubi E., Jodeh S., Lamhamdi A., Rodriguez-Castellón E., Algarra M., Zarrouk A., Errich A., Salghi R., Lgaz H. (2017) Eco friendly green inhibitor Gum Arabic (GA) for the corrosion control of mild steel in hydrochloric acid medium, *Corrosion Science*, 129, 2017, 70-81, ISSN 0010-938X, https://doi.org/10.1016/j.corsci.2017.09.027

Belghiti M.E., Karzazi Y., Dafali A., Obot I.B., *et al.* (2016) Anti-corrosive properties of 4-amino-3,5-bis(disubstituted)-1,2,4-triazole derivatives on mild steel corrosion in 2M H_3PO_4 solution: Experimental and theoretical studies, *Journal of Molecular Liquids*, 216, 874-886, ISSN 0167-7322, https://doi.org/10.1016/j.molliq.2015.12.093

Chauhan, D.S. Quraishi, M.A. and Qurashi, A. (2021). Recent trends in environmentally sustainable Sweet corrosion inhibitors, *J. Mol. Liq.* 326, 115117.

Deng S., Li X. and Xie X. (2014). Hydroxymethyl urea and 1, 3-bis (hydroxymethyl) urea as corrosion inhibitors for steel in HCl solution, *Corros. Sci.* 80, 276–289. https://doi.org/10.1016/j.corsci.2013.11.041

Dohare, P., Quraishi, M.A., Verma, C., Lgaz, H., Salghi, R. and Ebenso, E.E. (2019) Ultrasound induced green synthesis of pyrazolo-pyridines as novel corrosion inhibitors useful for industrial pickling process: Experimental and theoretical approach, *Results Phys.* 13, 102344.

Ebenso, E.E., Isabirye, D.A. and Eddy, N.O. (2010). Adsorption and quantum chemical studies on the inhibition potentials of some thiosemicarbazides for the corrosion of mild steel in acidic medium, *Int. J. Mol. Sci.* 11, 2473–2498. https://doi.org/10.3390/ijms11062473

Eddy, N.O. (2010). Part 3. Theoretical study on some amino acids and their potential activity as corrosion inhibitors for mild steel in HCl, *Mol. Simul.* 36, 354–363. https://doi.org/10.1080/08927020903483270

Eddy, N.O. (2011). Experimental and theoretical studies on some amino acids and their potential activity as inhibitors for the corrosion of mild steel, part 2, *J. Adv. Res.* 2, 35–47. https://doi.org/10.1016/j.jare.2010.08.005

Eddy, N.O., Ebenso, E.E. and Ibok, U.J. (2010). Adsorption, synergistic inhibitive effect and quantum chemical studies of ampicillin (AMP) and halides for the corrosion of mild steel in H2SO4, *J. Appl. Electrochem*. 40, 445–456. https://doi.org/10.1007/s10800-009-0015-z

Eddy, N.O., Momoh-Yahaya, H. and Oguzie, E.E. (2015). Theoretical and experimental studies on the corrosion inhibition potentials of some purines for aluminum in 0.1 M HCl, *J. Adv. Res.* 6, 203–217. https://doi.org/10.1016/j.jare.2014.01.004

El Arrouji, S. Alaoui, K.I. Zerrouki, A. *et al.* (2016). The influence of some pyrazole derivatives on the corrosion behaviour of mild steel in 1M HCl solution, *J. Mater. Environ. Sci*. 7, 299–309.

El Arrouji, S., Karrouchi, K., Berisha, A., Alaoui, K.I., Warad, I., Rais, Z., Radi, S., Taleb, M. and Zarrouk, A.(2020). New pyrazole derivatives as effective corrosion inhibitors on steel-electrolyte interface in 1 M HCl: Electrochemical, surface morphological (SEM) and computational analysis, *Colloids Surfaces A Physicochem. Eng. Asp.* 604, 125-325.

El Ouadi Y., Lamsayah M., Bendaif H., *et al*. (2021). Electrochemical and theoretical considerations for interfacial adsorption of novel long chain acid pyrazole for mild steel conservation in 1M HCl medium, *Chem. Data Collect*. 31, 100638.

El-Etre, A.Y. (2008). Inhibition of C-steel corrosion in acidic solution using the aqueous extract of zallouh root, *Mater. Chem. Phys.* 108, 278–282.

Emranuzzaman, T., Kumar, S. and Vishwanatham, G. U. (2004). Synergistic effects of formaldehyde and alcoholic extract of plant leaves for protection of N80 steel in 15% HCl, *Corros. Eng. Sci. Technol.*, 39, 327–332. https://doi.org/10.1179/174327804X13181

Essien, K.E. and Abai, E.J. (2022). Corrosion Inhibition Potential of Two Isoxazole Derivatives: Experimental and Theoretical Analyses. *J. Mater. Environ. Sci.*, 13(08), 928-944.

Essien, K. E., BoEkom, E. J., Okon, O. E., Odiongenyi, A. O., George I. and Okon E. J. (2023). Investigation of Corrosion Inhibition behaviour of 3-Methyl-5-Phenylisoxazole on Mild Steel Surface in HCl Solution, *J. Mater. Environ. Sci.*, 14(7), 811-825.

Fouda, A.S., Abd El-Aal, A. and Kandil, A.B. (2006). The effect of some phthalimide derivatives on corrosion behavior of copper in nitric acid, *Desalination.* 201, 216–223. https://doi.org/10.1016/j.desal.2005.11.030

Ganesan, A.R., Subramani, K., *et al*. (2020). A comparison of nutritional value of underexploited edible seaweeds with recommended dietary allowances, *J. King Saud Univ.* 32,1206–1211.

Ghazoui A., Bencaht N., Al-Deyab S.S., Zarrouk A., *et al.* (2013), An Investigation of Two Novel Pyridazine Derivatives as Corrosion Inhibitor for C38 Steel in 1.0 M HCl, *Int. J. Electrochem. Sci.*, 8(2), 2272-2292

Glaser, R., Lewis, M. and Wu, Z.(2000). Stereochemistry and stereoelectronics of azines. 13. Conformational effects on the quadrupolarity of azines. An ab initio quantum-mechanical study of a lateral synthon, *Mol. Model. Annu*. 6, 86–98.

Hammouti B., Zarrouk A., Al-Deyab S.S., Warad I. (2011), Temperature effect, activation energies and thermodynamics of adsorption of ethyl 2-(4-(2-ethoxy-2-oxoethyl)-2-p-tolylquinoxalin-1(4H)-yl)acetate on Cu in HNO_3, *Oriental J. Chem.* 27(1), 23-31.

Hayaoui, M., Drissi, M., Fahim, M., *et al.* (2017). Benzenamine derivative as corrosion inhibitor of carbon steel in hydrochloric acid solution: electrochemical and theoretical studies, *J. Mater. Environ. Sci.*, 8(5), 1877.

Hosseini, M.G., Ehteshamzadeh, M. and Shahrabi, T. (2007). Protection of mild steel corrosion with Schiff bases in 0.5 M H2SO4 solution, *Electrochim. Acta.* 52, 3680–3685.

Hosseini, S.M., Salari, M., Jamalizadeh, E., Khezripoor, S. and Seifi, M.(2010). Inhibition of mild steel corrosion in sulfuric acid by some newly synthesized organic compounds, *Mater. Chem. Phys*. 119, 100–105. https://doi.org/10.1016/j.matchemphys.2009.08.029

Hmamou D. B., Salghi R., Zarrouk A. (2015). Investigation of corrosion inhibition of carbon steel in 0.5 M H_2SO_4 by new bipyrazole derivative using experimental and theoretical approaches, *Journal of Environmental Chemical Engineering*, 3 N°3, 2031-2041

Ikot, A. N., Akpabio, L. E., Essien, K., Ituen E. E. and Obot. I. B. (2009). Variational Principle Techniques and the Properties of a Cut-off and Anharmonic Wave Function, *E-Journal of Chemistry*, 6(1), 113-119.

Ishii, M., Nakahira, M. and Yamanaka, T.(1972). Infrared absorption spectra and cation distributions in $(Mn, Fe)_3O_4$, *Solid State Commun*. 11, 209–212

Jackson, E. and Essien, K.E. (2019). Experimental and Theoretical Approach of L-Methionine Sulfone (LMS) as corrosion inhibitor for mild steel in HCL Solution, *Environment.*,1, 2.

Khaled, K.F., Abdel-Rehim, S.S. and Sakr, G.B. (2012). On the corrosion inhibition of iron in hydrochloric acid solutions, Part I: Electrochemical DC and AC studies, *Arab. J. Chem*. 5, 213–218. https://doi.org/10.1016/j.arabjc.2010.08.015

Kousar K., Walczak M.S., Ljungdahl T., *et al*. (2021). Corrosion inhibition of carbon steel in hydrochloric acid: Elucidating the performance of an imidazoline-based surfactant, *Corros. Sci.* 180, 109195.

Le Goff, G. and Ouazzani, J. (2014). Natural hydrazine-containing compounds: Biosynthesis, isolation, biological activities and synthesis, *Bioorg. Med. Chem.* 22, 6529–6544.

Li X., Deng S., Xie X. and Fu H. (2014). Inhibition effect of bamboo leaves' extract on steel and zinc in citric acid solution, *Corros. Sci.* 87, 15–26. https://doi.org/10.1016/j.corsci.2014.05.013

Misawa,T., Asami K., Hashimoto K. and Shimodaira S. (1974). The mechanism of atmospheric rusting and the protective amorphous rust on low alloy steel, *Corros. Sci.* 14, 279–289.

Misawa T., Kyuno T., Suetaka W. and Shimodaira S. (1971). The mechanism of atmospheric rusting and the effect of Cu and P on the rust formation of low alloy steels, *Corros. Sci.* 11, 35–48.

Njoku, D.I., Onuoha, G.N., Oguzie, E.E., Oguzie, K.L., Egbedina, A.A. and Alshawabkeh, A.N. (2019). Nicotiana tabacum leaf extract protects aluminium alloy AA3003 from acid attack, *Arab. J. Chem*. 12, 4466–4478. https://doi.org/10.1016/j.arabjc.2016.07.017

Obi-Egbedi, N.O., Essien, K.E. and Obot, I.B. (2011). Computational simulation and corrosion inhibitive potential of alloxazine for mild steel in 1M HCl, *J. Comput. Methods Mol. Des.* 1, 26–43.

Obi-Egbedi, N.O., Essien, K.E., Obot, I.B. and Ebenso, E.E. (2011).1, 2-Diaminoanthraquinone as corrosion inhibitor for mild steel in hydrochloric acid: weight loss and quantum chemical study, *Int. J. Electrochem. Sci.* 6, 913–930.

Obot A.S., BoEkom E.J., Ituen E.B., Ugi B.U., Essien K.E. and Jonah N.B. (2021). Thermodynamic investigation and quantum chemical evaluation of n-hexane extracts of Costus lucanusianus as corrosion inhibitors for mild steel and aluminum in 1 m hcl solution, *J. Appl. Phys. Sci. Int.* 13, 6–27.

Obot, I.B. Obi-Egbedi, N.O. (2008). Fluconazole as an inhibitor for aluminium corrosion in 0.1 M HCl, Colloids Surfaces a Physicochem. *Eng. Asp.* 330, 207–212. https://doi.org/10.1016/j.colsurfa.2008.07.058

Obot, I.B., Obi-Egbedi, N.O. and Odozi, N.W. (2010). Acenaphtho [1, 2-b] quinoxaline as a novel corrosion inhibitor for mild steel in 0.5 M H_2SO_4, *Corros. Sci.* 52, 923–926. https://doi.org/10.1016/j.corsci.2009.11.013

Oguzie, E.E., Adindu, C.B., Enenebeaku, C.K., Ogukwe, C.E., Chidiebere, M.A. and Oguzie, K.L. (2012). Natural products for materials protection: mechanism of corrosion inhibition of mild steel by acid extracts of Piper guineense, *J. Phys. Chem. C.* 116, 13603–13615. https://doi.org/10.1021/jp300791s

Ouafi A., Hammouti B., Oudda H., Kertit S., Touzani R., Ramdani A. (2002), New pyrazole derivatives as effective Inhibitors for the corrosion of mild steel in HCl medium, *Anti-Corros. Meth. Mater.* 49 N°3, 199-204.

Ouchrif A., Zegmout M., Hammouti B., El-Kadiri S. Ramdani A. (2005). 1,3-Bis(3-hyroxymethyl-5-methyl-1-pyrazole) propane as corrosion inhibitor for steel in 0.5 M H_2SO_4 solution, *Appl. Surf. Sci.* 252, 339–344.

Ozoemena, C. P., Boekom, E. J., Abai, E. J., *et al.* (2023). Schiff Base and Its Metal Complexes as Ecofriendly PittingCorrosion Inhibitors on ASTM-A36 Low Carbon Steel in Corrosive Oil and Gas Well Treatment Fluids, *Science Journal of Chemistry,* 11(5): 168-188.

Paul, P.K., Yadav, M. and Obot, I.B. (2020). Investigation on corrosion protection behavior and adsorption of carbohydrazide-pyrazole compounds on mild steel in 15% HCl solution: Electrochemical and computational approach, *J. Mol. Liq.*, 314, 113513.

Salim, R., Ech-chihbi, E., Oudda, H., *et al.* (2016). The inhibition effect of imidazopyridine derivatives on C38 steel in hydrochloric acid solution, *Der Pharma Chem.*, 8(3), 200.

Sastri, V.S. (2012). Green corrosion inhibitors: theory and practice, John Wiley & Sons. ISBN: 978-1-118-01541-4

Solomon, M.M., Essien, K.E., Loto, R.T. and Ademosun, O.T. (2022). Synergistic corrosion inhibition of low carbon steel in HCl and H2SO4 media by 5-methyl-3-phenylisoxazole-4-carboxylic acid and iodide ions, *J. Adhes. Sci. Technol.* 36, 1200–1226.

Soltani, N., Tavakkoli, N., Kashani, M.K., Mosavizadeh, A., Oguzie, E.E. and Jalali, M.R. (2014). Silybum marianum extract as a natural source inhibitor for 304 stainless steel corrosion in 1.0 M HCl, *J. Ind. Eng. Chem.* 20, 3217–3227. https://doi.org/10.1016/j.jiec.2013.12.002

Tang, L., Li, X., Mu, G., Liu, G., Li, L., Liu, H. and Si, Y. (2006). The synergistic inhibition between hexadecyl trimethyl ammonium bromide (HTAB) and NaBr for the corrosion of cold rolled steel in 0.5 M sulfuric acid, *J. Mater. Sci.* 41,3063–3069. https://doi.org/10.1007/s10853-006-6987-8

Tebbji K., Bouabdellah I., Aouniti A., *et al.* (2007), N-benzyl-N,N-bis[(3,5-dimethyl-1H-pyrazol-1-yl)methyl]amine as corrosion inhibitor of steel in 1 M HCl, *Mater. Let.* 61N°3, 799-804.

Thoume, A., Elmakssoudi, A., Left, D.B., *et al.* (2020). Amino acid structure analog as a corrosion inhibitor of carbon steel in 0.5 M H2SO4: Electrochemical, synergistic effect and theoretical studies, *Chem. Data Collect.* 30, 100586.

Umoren, S.A. (2008). Inhibition of aluminium and mild steel corrosion in acidic medium using Gum Arabic, *Cellulose.* 15, 751–761. https://doi.org/10.1007/s10570-008-9226-4

Umoren, S.A. (2011). Synergistic inhibition effect of polyethylene glycol–polyvinyl pyrrolidone blends for mild steel corrosion in sulphuric acid medium, *J. Appl. Polym. Sci.* 119, 2072–2084. https://doi.org/10.1002/app.32922

Verma, C. Saji, V.S. Quraishi, M.A. and Ebenso, E.E. (2020). Pyrazole derivatives as environmental benign acid corrosion inhibitors for mild steel: experimental and computational studies, *J. Mol. Liq.* 298, 111943.

Yadav M. Gope L. Kumari N. and Yadav P. (2016). Corrosion inhibition performance of pyranopyrazole derivatives for mild steel in HCl solution: Gravimetric, electrochemical and DFT studies, *J. Mol. Liq.* 216, 78–86.

Yadav, M., Behera, D. and Kumar, S. (2014). Experimental and theoretical studies on corrosion inhibition of mild steel in hydrochloric acid by thiosemicarbazone of Schiff bases, *Can. Metall. Q.* 53, 220–231. https://doi.org/10.1179/1879139513Y.0000000118

Zarrok H., Zarrouk A., Salghi R., Oudda H., *et al.* (2012) Gravimetric and quantum chemical studies of 1-[4-acetyl-2-(4-chlorophenyl)quinoxalin-1(4H)-yl]acetone as corrosion inhibitor for carbon steel in hydrochloric acid solution,, *J. Chem. Pharmac. Res.*, 4 N°12, 5056-5066

Zarrouk A., Hammouti B., Zarrok H., Al-Deyab S.S., Messali M. (2011) Temperature effect, activation energies and thermodynamic adsorption studies of L-cysteine Methyl ester hydrochloride as copper corrosion inhibitor in nitric acid 2M, *Int. J. Electrochem. Sci.*, 6(12), 6261-6274